Lag Times Associated With Fire Detection and Suppression

Frederick W. Mowrer*

Abstract

The effectiveness of fire detection systems and fire mitigation strategies can be related to three distinct time lags associated with building fires: a transport time lag, a detection time lag, and a suppression time lag. The impacts of these lag periods on fire detection and suppression are developed. Transport lag periods are considered in terms of available correlations of fire plume and ceiling jet data, detection lag periods in terms of available heat detector response models that use these data correlations. Suppression lags are developed in terms of expected response times for automatic and manual suppression. Example calculations are presented.

Introduction

Calculation of the response of fire detectors, sprinklers, and other heat-sensitive objects located at ceiling level requires a knowledge of the fire environment to which these elements are exposed. Currently, such information is available for large spaces with flat, unobstructed ceilings in terms of temperature and velocity correlations for fire plumes and ceiling jets. Correlations currently utilized to describe the fire environment at detectors are reviewed, and the relationship between the available t-squared and quasi-steady correlations is developed.

The response of fire detection devices and fire suppression systems can be evaluated in terms of three distinct lag periods: a transport time lag, a detection time lag, and a suppression time lag. Transport lags are considered here within the context of the available data correlations, while detection lags are developed in terms of available detector response models that use these data correlations. Suppression lags are

---

Key words: Fire plumes; ceiling jets; detection; suppression; response time.

*Department of Fire Protection Engineering, University of Maryland, College Park, Maryland 20742.

considered in terms of expected response times for automatic and manual suppression systems. The overall impact of these lag periods on the response of fire detectors and on the formulation of fire mitigation strategies is developed. Example calculations are presented to illustrate these influences.

Review of Fire Plume/Ceiling Jet Data Correlations

Available fire plume and ceiling jet data correlations are of two types: quasi-steady and power law. Quasi-steady correlations are based on fire experiments with heat release rates that do not vary appreciably with time; power law correlations are based on fires characterized with heat release rates that grow as a power of the time from ignition. The primary focus here is on the relationship between these two types of correlations and on the use of these correlations for fire detection analysis. Data correlations of Alpert ,[1] Heskestad and Delichatsios (H&D),[2] and Alpert and Ward (A&W)[3] are used for this discussion. Beyler[4] has compiled a comprehensive review of available fire plume and ceiling jet data correlations.

Alpert developed the original of these correlations based on large-scale quasi-steady fire experiments, while Heskestad and Delichatsios have developed correlations for both quasi-steady fires as well as power law fires. More recently, Alpert and Ward have suggested new coefficients for the original Alpert correlation. These new coefficients produce results closer to the quasi-steady correlation of Heskestad and Delichatsios.

Quasi-steady Fires

Plume theory[5] suggests that the maximum temperature rise above ambient of a plume of hot gases rising from a point source of heat can be expressed with an equation of the form:

$$dT = k_T Q^{2/3} / H^{5/3} \tag{1}$$

where:

dT = Temperature rise above ambient (K)
k_T = Temperature coefficient
Q = Heat release rate of fire (kW)
H = Height above plume source (m).

Available correlations of fire plume data have been developed in this form.

The theory of ceiling jet flows is more complicated, as evidenced by

Alpert's[6] detailed analysis of this region. It involves consideration of the rate of entrainment into the ceiling jet as well as the viscous effects and heat transfer associated with the flow of buoyant gases beneath and in contact with the ceiling. The maximum temperature rise occurs within the area where the fire plume impinges the ceiling and falls off as a function of the radius beyond this zone. The ceiling jet data correlations of Alpert, Heskestad and Delichatsios, and Alpert and Ward can all be expressed in the form of Equation 1, but in the ceiling jet region, the coefficient k_T is also a function of the nondimensional radial distance from the plume centerline, r/H, to account for the temperature decay that occurs with increasing distance from the plume impingement region. Similarly, plume theory suggests that gas velocity in the plume region has the form:

$$U = k_u (Q/H)^{1/3} \tag{2}$$

where:

U = Fire gas velocity (m/s)
k_u = Velocity correlation coefficient.

As with the temperature data, the velocity correlation coefficient, k_u, is expected to fall off as a function of the radial distance from the plume. Available velocity correlations have this characteristic form.

The coefficients, k_T and k_u, for the quasi-steady temperature and velocity data correlations of Alpert, Heskestad and Delichatsios, and Alpert and Ward are tabulated in Table 1. Where available, recommendations of Beyler, based on his review, also are tabulated. Normalized curves are illustrated in Figures 1a and 1b, which show the nondimensional temperature rise, dT^*, and velocity, U^*, respectively, as functions of the nondimensional radial distance, r/H, from the plume centerline. Two regions are used to correlate the data: a plume impingement region and a ceiling jet region. The plume impingement region occurs within a radius of approximately $0.2\ H\ (r/H < 0.2)$.

The correlation coefficients provided in Table 1 are based on theoretical total heat release rates, which are determined as the product of the fuel mass loss rate and the theoretical heat of combustion. The heat release rate actually contributing to the velocities and temperatures in the plume and in the ceiling jet is the convective heat release rate. The convective heat release rate differs from the total theoretical heat release rate because of combustion inefficiency and radiative losses from the fire source. This can be expressed as:

$$Q_c = x_a (1 - x_r) Q_t \tag{3}$$

Table 1: Quasi-steady correlations.

a. Temperature correlations: $dT = k_T Q^{2/3}/H^{5/3}$

	Values for k_T	
	Plume	Ceiling jet
Alpert	16.9	$5.4/(r/H)^{2/3}$
Heskestad and Delichatsios	$2.75/D^{4/3}$	$2.75/D^{4/3}$
Alpert and Ward	22.0	$6.8/(r/H)^{2/3}$
Beyler recommendation	22.0	H&D correlation

b. Velocity correlations: $U = k_u (Q/H)^{1/3}$

	Values for k_u	
	Plume	Ceiling jet
Alpert	0.95	$0.2/(r/H)^{5/6}$
Heskestad and Delichatsios	None	$0.21/[(r/H)^{0.63} D^{2/3}]$
Beyler recommendation	1.04	
$D = 0.25$	$r/H < 0.2$	
$D = 0.188 + 0.313\, r/H$	$r/H > 0.2$	

where:

Q_c = Convective heat release rate (kW)
x_a = Combustion efficiency factor (Q_a/Q_t)
x_r = Radiative fraction of actual heat release rate (Q_r/Q_a)
Q_t = Total theoretical heat release rate (kW)
Q_a = Total actual heat release rate (kW).

The ratio of the convective to theoretical heat release rate, Q_c/Q_t, is expected to remain fairly constant for a given material, but can vary considerably among different materials.[7] For wood, which serves as the primary basis for the available correlations, Heskestad and Delichatsios[8] suggest this ratio has a value of about 0.45. Adjustments should be made for application of the correlations to materials with convective ratios considerably different from this value. Tewarson[9] provides convective ratio data, measured in small-scale tests, for a range of materials.

According to Alpert and Ward, these correlations provide reasonable accuracy for predicted temperatures between approximately 70°C and 850°C (150–1500°F). Predicted temperatures above 850oC indicate the likelihood of flame at the location being evaluated. The low temperature

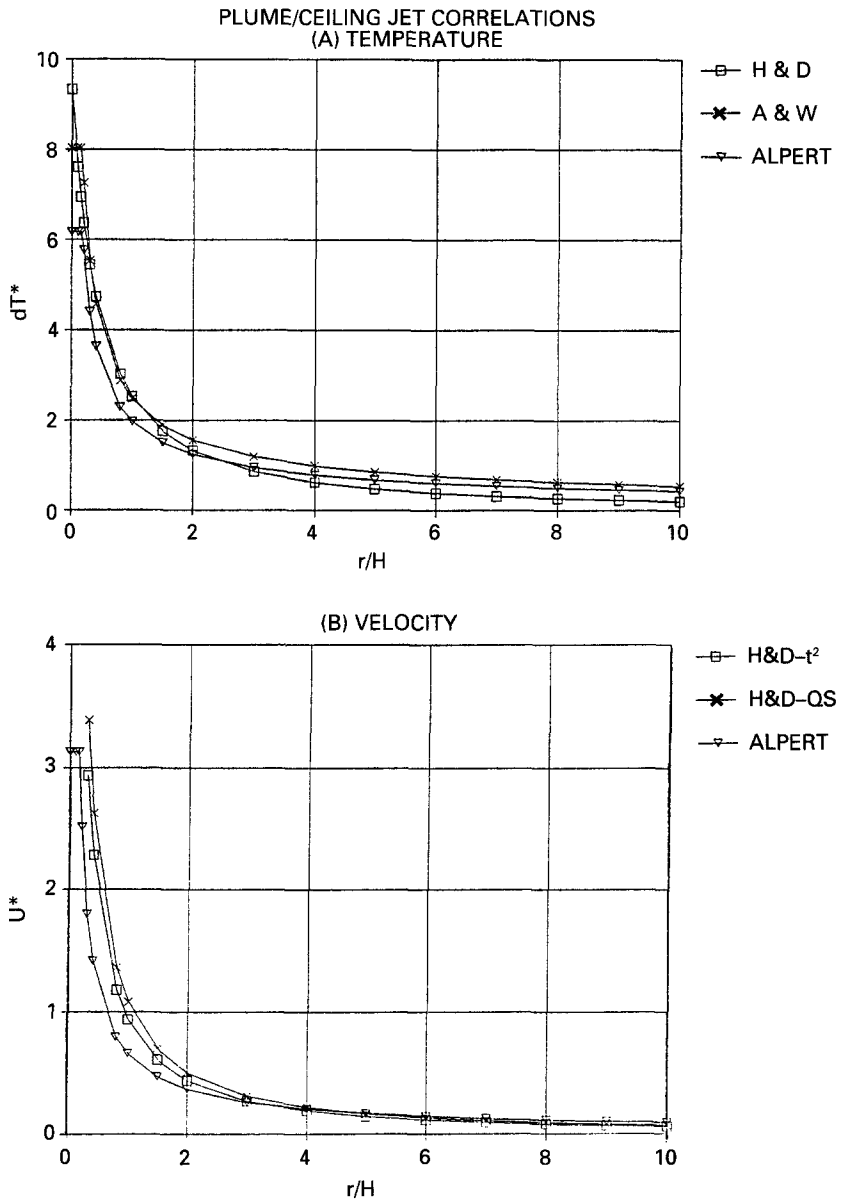

Figure 1. Illustration of the plume/ceiling jet correlations of Alpert (Alpert), Alpert and Ward (A&W), and Heskestad, and Delichatsios (H&D); (a) nondimensional temperature rise versus nondimensional radial distance, r/H, from the plume centerline, and (b) nondimensional velocity versus radial distance.

extreme is not representative of a threat to the building structure, so better accuracy is not normally warranted unless nonthermal damage is of interest.

Power Law Fires

Heskestad and Delichatsios also have correlated temperature and velocity relationships for idealized, yet realistic, classes of fires referred to as "power-law" fires because the heat release rate is considered to grow as some power of time:

$$Q = \alpha (t - t_o)^p \tag{4}$$

where:

α = Power law fire growth coefficient (kW/s^p)
t = Time from ignition (s)
t_o = Incubation time offset (s)
p = Fire growth exponent.

This equation can be applied to either theoretical or convective heat release rates, provided appropriate values of α are used in conjunction with either the theoretical or convective heat release rate. The relationship between convective and total theoretical growth coefficients is the same as that between convective and theoretical heat release rates expressed in Equation 3:

$$\alpha_c = x_a (1 - x_r) \alpha_t \tag{5}$$

For this class of fire characterizations, Heskestad and Delichatsios developed nondimensional correlations of the form:

$$dT^*_p = \{gH^{(7-p)/(3+p)} / [A\alpha H]^{2/(3+p)}\} (dT / T_o) \tag{6}$$

$$U^*_p = \{(H^{(2-p)/(p+3)} / [A\alpha H]^{1/(3+p)}\} U \tag{7}$$

$$t^*_p = \{[A\alpha H]^{1/(3+p)} / H^{5/(3+p)}\} t \tag{8}$$

where:

dT^*p = Nondimensional temperature rise above ambient
U^*_p = Nondimensional velocity
t^*_p = Nondimensional time
g = Gravitational constant (9.8 m/s^2)
$A = g/(c\, p_o\, T_o)$ = (0.028 m^2/kg or m^4/kWs^3)
T_o = Ambient temperature (298 K).

For the case of parabolic fire growth ($p = 2$), which has become widely used to represent a range of realistic fire growth rates, these relationships reduce to:

$$dT^*_2 = \{gH/[A\alpha H]^{2/5}\}\,(dT/T_o) \tag{9}$$

$$U^*_2 = \{1/[A\alpha H]^{1/5}\}\,U \tag{10}$$

$$t^*_2 = \{[A\alpha H]^{1/5}/H\}\,t \tag{11}$$

The t-squared temperature and velocity correlations originally developed by Heskestad and Delichatsios use the total theoretical heat release rate. These correlations, based on large-scale experiments with wood cribs, are:

$dT^*_2 = 0$ for $t^*_2 \le t^*_{2f}$; and

$$dT^*_2 = [\,(t^*_2 - t^*_{2f})\,/\,D\,]^{4/3} \text{ for } t^*_2 > t^*_{2f} \tag{12}$$

$$U^*_2 / \sqrt{dT^*_2} = 0.59\,/\,(r/H)^{0.63} \tag{13}$$

$$t^*_{2f} = 0.954\,(1 + r/H) \tag{14}$$

where:

D = Nondimensional distance parameter
= 0.25 for $r/H < 0.2$; and
= $0.188 + 0.313\,r/H$; for $r/H > 0.2$

t^*_{2f} = Nondimensional transport time lag parameter.

Appropriate values for α_t must be substituted into Equations 9-11 to use the correlations in this form.

Recently, Heskestad and Delichatsios[8] have restructured their original correlations in terms of the convective heat release rate rather than the total theoretical heat release rate. These generalized correlations, which permit direct application to combustibles with convective fractions significantly different from wood, are expressed as:

$dT^*_2 = 0$ for $t^*_{2c} \le t^*_{2fc}$; and

$$dT^*_2 = [\,(t^*_{2c} - t^*_{2fc})\,/\,D_c\,]^{4/3}\,; \text{ for } t^*_{2c} > t^*_{2fc} \tag{15}$$

$$U^*_{2c} / \sqrt{dT^*_{2c}} = 0.59\,/\,(r/H)^{0.63} \tag{16}$$

$$t^*_{2fc} = 0.813\,(1 + r/H) \tag{17}$$

where:

D_c = Nondimensional distance parameter
= 0.17 for $r/H < 0.2$
= 0.126 + 0.210 r/H for $r/H > 0.2$
t^*_{2fc} = Nondimensional transport time lag parameter.

These correlations have the same form as the original ones, but the coefficients are different to account for the difference between convective and total theoretical heat release rates. Appropriate values for α_c must be substituted into Equations 9–11 to use the correlations in the forms of Equations 15–17. These nondimensional forms are useful for the correlation of data over a wide range of fire test conditions, but they are cumbersome for engineering calculations. For engineering use and for comparison with the quasi-steady correlations, it is useful to rewrite the t-squared correlations of Heskestad and Delichatsios in dimensional form as:

$$dT = 0 \text{ for } t < t_l; \text{ and} \tag{18a}$$

$$dT = (A^{2/3}/gD^{4/3})T_o\, Q_s^{2/3}/H^{5/3} \text{ for } t > t_l \tag{18b}$$

For representative values of A, g, and T_o, this evaluates to:

$$dT = (2.75/D^{4/3})\, Q_s^{2/3}/H^{5/3} \text{ for } t > t_l \tag{18c}$$

$$U = [0.18/[(r/H)^{0.63}\, D^{2/3}]]\,(Q_s/H)^{1/3} \tag{19}$$

where:

t_l = Transport time lag (s)
Q_s = Sensed heat release rate (kW).

These dimensional forms apply to both the original and convective correlations of Heskestad and Delichatsios, provided appropriate values for D, Q_s, and t_l are used.

The Relationship Between Quasi-steady and t^2 Correlations

The temperature correlation expressed by Equation 18c is identical to the quasi-steady correlation of Heskestad and Delichatsios once the instantaneous heat release rate, $Q(t)$, at any time is replaced by the heat release rate sensed at the location of interest, $Q_s(t)$, at that time. The

difference between these terms can be considered in terms of a simple translation along the time axis equal to the transport time lag:

$$Q_s(t) = 0 \text{ for } t < t_l \text{; and}$$

$$Q_s(t) = Q\,(t - t_l) \text{ for } t > t_l \qquad (20)$$

Equation 20 applies to either the original or convective correlations, depending on which value of Q is specified. To use the original correlation, Q_t is substituted for Q; to use the convective correlation, Q_c is substituted for Q. The topic of transport time lags is developed in the next section.

The t-squared velocity correlation has the same functional form as the quasi-steady correlation, but has a magnitude approximately 15 percent less than the quasi-steady correlation. These similarities are more than fortuitous; Heskestad and Delichatsios formulated their t-squared correlation to asymptotically approach the quasi-steady limit.

The difference between the instantaneous heat release rate and the heat release rate sensed at a location is a function of the distance from the fire source to the location and the transport speed of the fire gases. For the t-squared correlations, this transport speed is expressed in terms of the parabolic fire growth coefficient, α. As developed in the next section, the difference between the instantaneous and sensed heat release rates can be significant and, according to the t-squared correlation, this difference continues to grow as long as the fire continues to grow parabolically.

Lag Times Associated With Fires

The potential for manual or automatic fire control based on the operation of fire detection and suppression systems relates directly to three distinct delay periods between fire initiation and the start of suppression. These three periods can be considered as (1) a transport time lag, t_l; (2) a detection time lag, t_d; (3) a suppression time lag, t_s.

The transport time lag, t_l, represents the time between the actual generation of heat or another fire signature and the transport of that signature to the fire detection device. The detection time delay, t_d, represents the time period from the first transport of a fire signature to a sprinkler or fire detector until the device actuates. The final lag period, the suppression time lag, t_s, represents the time from fire detection until the initiation of fire suppressant application. These periods are similar to ones suggested by Johnson[10] and by Newman.[11]

These three lag periods are illustrated schematically in Figure 2 for an idealized heat release history. The idealized fire history without suppression illustrates a period of accelerating fire growth, followed by

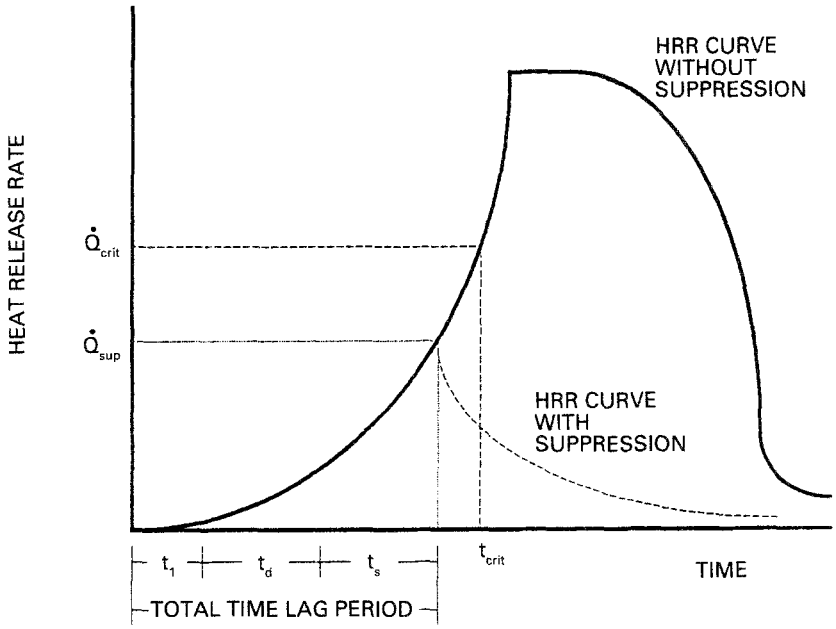

Figure 2. Schematic illustration of the influence of transport, detection, and suppression lag periods in terms of a representative heat release rate curve.

a period of steady heat release rate associated with full involvement of a burning object or room. The decay period that follows this steady period would be associated with fuel burnout in the absence of any fire suppression activity.

The suppression curve in Figure 2 illustrates an example of satisfactory performance because the total lag period is less than the time to critical damage. Unsatisfactory performance would result for situations where the total lag period exceeds the time to critical damage. To use this concept of performance-based criteria, the time to critical damage must be established by appropriate analyses of the expected rate of hazard development and the response of building systems, contents, and occupants to this development. For this example, the critical time is represented in terms of a critical heat release rate.

Transport Time Lags

Upon preliminary inspection of Figure 2, the transport lag does not appear to be important because it is represented at the start of a fire, before the heat release rate has grown to significant levels. But the influence of the transport lag propagates through the fire growth period. As illustrated in Figure 3, the heat release rate being sensed at a detector can lag the actual heat release rate by a significant margin. This

difference continues to grow as long as the fire continues to grow. The longer the three lag periods are, the larger this margin will be. The detector responds to the heat release rate sensed at the detector, while it is the actual heat release rate of the fire that must be suppressed.

Transport Lags Associated with t^2 Correlations

The t-squared correlation of Heskestad and Delichatsios considers the transport lag explicitly. The heat release rate sensed at a location in a fire plume or ceiling jet, Q_s, lags the instantaneous heat release rate by a transport lag time, t_l. This can be expressed as:

$$Q_s = 0 \text{ for } t \leq t_l \text{; and}$$

$$Q_s = \alpha (t - t_l)^2 \text{ for } t > t_l \qquad (21)$$

This can be applied to either the original or the convective correlations through use of appropriate α and t_l values.

The relationship between the instantaneous and sensed heat release rates for t-squared fire representations is illustrated in dimensionless terms in Figure 3. The curves differ only by a translation along the time axis equal to the transport time lag. Once this transport lag is considered, there is no difference between the quasi-steady and t-squared

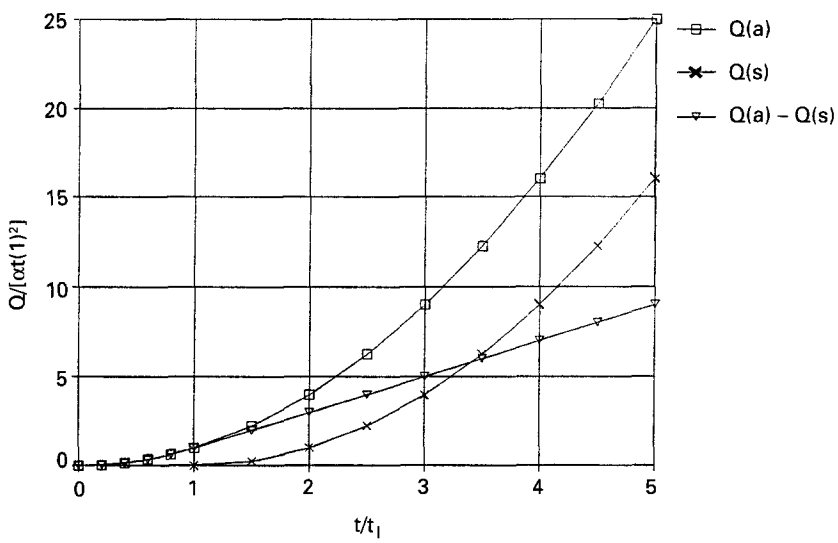

Figure 3. Illustration of the influence of the transport time lag on the response of thermal detectors to t-squared fires.

temperature correlations of Heskestad and Delichatsios.

The difference between the instantaneous and sensed heat release rates continues to grow with time. The rate by which the sensed heat release rate lags the instantaneous heat release rate can be expressed for t-squared fires as:

$$Q_l \,/\, \alpha t_l^2 = (t/t_l)^2 \text{ for } t < t_l \text{; and}$$

$$Q_l \,/\, \alpha t_l^2 = (2t \,/\, t_l - 1) \text{ for } t > t_l \qquad (22)$$

This relationship is illustrated in Figure 3, where Q_a is the actual instantaneous heat release rate at any time, Q_s is the sensed heat release rate at any time, and Q_l is the difference between Q_a and Q_s. The longer the transport lag, the larger the lag will be between the instantaneous heat release rate and the sensed heat release rate at any time.

According to the Heskestad and Delichatsios correlations for t-squared fires, transport time lags can be calculated as:

$$t_l = [0.954\,(H + r)]/(A\alpha_t H)^{1/5}\ s \qquad (23a)$$

$$= [0.813\,(H + r)]/(A\alpha_c H)^{1/5}\ s \qquad (23b)$$

The term $(H + r)$ is the characteristic distance traveled by fire gases from the fire source to the ceiling location of interest. The term $(A\alpha H)^{1/5}$ has units of m/s and can be interpreted as a characteristic velocity of the fire gases.

Newman[11] suggests an alternative expression, based on a data correlation and applicable to power law fires, for calculating transport time lags:

$$t_l = \{1.4\,(r/H) + 0.2\}\,[H^5/(A\alpha_t H)]^{1/(3+p)} \qquad (24)$$

For t-squared fires ($p = 2$), this expression evaluates as:

$$t_l = \{1.4\,(r/H) + 0.2\}\,[H^5/(A\alpha_t H)]^{1/5} \qquad (25a)$$

$$= (1.4r + 0.2H)/(A\alpha_t H)^{1/5} \qquad (25b)$$

Newman's correlation for the transport time lag in t-squared fires (Equation 25b) makes more physical sense than the transport lag correlation of Heskestad and Delichatsios because it recognizes the difference between the average transport velocities in the plume and ceiling jet regions. Newman's correlation approximates this difference,

illustrated in Figure 1b, to be a velocity in the plume region that is seven times higher than in the ceiling jet region. While not exact because of the variable velocities in the ceiling jet region, this difference is consistent with the plume and ceiling jet velocities illustrated in Figure 1b.

Transport Lags Associated with Quasi-steady Correlations

The quasi-steady temperature and velocity correlations do not consider transport lags explicitly. Effects of the actual heat release are considered to propagate instantly throughout the fire plume and ceiling jet. The transport time lag for quasi-steady fires can be estimated to permit evaluation of its importance for different scenarios. The transport time lag can be calculated generally as:

$$t_l = d/\bar{u} \tag{26}$$

where:

d = Distance traveled by the fire gases (m)
$\bar{u}$ = Average velocity of fire gases over distance d (m/s) .

Within the plume region, the distance traveled by fire gases, d, is simply the height H from the fire source to the location being considered. Average velocity in the plume is calculated, using $u(z) = 1.0\,(Q_t/z)^{1/3}$, as:

$$\bar{u}_{pl} = \frac{1}{H}\int_0^H u\,(z)\,dz = \frac{1}{H}\int_0^H \left[\,1.0\left(\frac{Q_t}{z}\right)^{\frac{1}{3}}\right] dz = 1.5\,u\,(H) \tag{27}$$

The average velocity over the height H is 1.5 times the local velocity at H. Therefore, within the plume region, the transport time lag can be evaluated as:

$$t_{tpl} = H/[1.5\,u(H)] \tag{28a}$$

$$= 0.67\,H^{4/3}/Q_t^{1/3} \tag{28b}$$

The transport time lag within the ceiling jet region is the plume transport lag plus the transport lag within the ceiling jet. The distance traveled by gases in the ceiling jet is the radial distance R from the plume centerline to the object under consideration. Using Alpert's correlation for ceiling jet velocities, the average velocity of the jet is evaluated as:

$$\bar{u}_{cj} = \frac{1}{R}\int_0^P u\,(r)\,dr = \frac{1}{R}\int_0^P \left[\,0.2\left(\frac{Q_t}{H}\right)^{\frac{1}{3}} / \left(\frac{r}{H}\right)^{\frac{5}{6}}\right] dr = 6\,u\,(R) \tag{29}$$

Consequently, the transport time lag within the ceiling jet can be evaluated as:

$$t_{l,cj} = R/[6\ u(R)] \tag{30a}$$

$$= R^{11/6} / [1.2\ Q_t^{1/3} H^{1/2}] \tag{30b}$$

The total time lag for the ceiling jet region then is evaluated as:

$$t_{l,tot} = t_{l,pl} + t_{l,cj} \tag{31}$$

For heat release rates that vary with time, this analysis of quasi-steady fires suggests that the transport time lag also will vary with time. For example, if a t-squared representation of the heat release rate ($Q = \alpha t^2$) is substituted for Q into Equations 28 and 30, this time dependence is illustrated. Thus, due to differences in the forms of the quasi-steady and t-squared representations, they are not expected to yield identical results even if a transport time lag is added to the quasi-steady correlation.

The Newman correlation for transport time lags expressed by Equation 24 can also be applied to the case of quasi-steady fires by setting $p = 0$ and $\alpha = Q$. For this case, Equation 24 evaluates as:

$$t_l = \{1.4\ (r/H) + 0.2\}\ H^{5/3}/(AQH)^{1/3} \tag{32}$$

which can be separated into plume and ceiling jet regions:

$$t_{l,pl} = 0.2\ H^{5/3} / (AQH)^{1/3} \tag{33a}$$

$$= 0.66\ H^{4/3} / Q^{1/3} \tag{33b}$$

$$t_{l,cj} = (1.4\ r/H)\ H^{5/3} / (AQH)^{1/3} \tag{34a}$$

$$= 4.61\ r / (Q/H)^{1/3} \tag{34b}$$

Thus, Newman's expression for the plume region transport lag is virtually identical to the one derived here and expressed by Equation 28b if the theoretical heat release rate is used.

Newman's expression for the ceiling jet transport lag differs in form from the one derived here; his expression demonstrates a first power dependence of the transport lag on radial distance, while the one derived here demonstrates almost a second power relationship. This difference is most likely due to the difference in form between the Alpert and the

Heskestad and Delichatsios velocity correlations in the ceiling jet region (see Table 1). The form derived here is more consistent with the decaying nature of the velocity as a function of radial distance in the ceiling jet region. But over radial distances normally of interest, either form should suffice.

Detection Time Lags

The detection time lag depends on the fire environment history at the detector and on the response characteristics of the device. For detection, a threshold magnitude of the fire signature being detected must be transported to the detector and maintained for a sufficiently long period to overcome inertial effects in the detector. Newman[12] discusses the methods available to evaluate these parameters for a range of detection devices. In this paper, models of heat detector response are used to illustrate the concept of detection time lags.

The DETACT models[13,14] of detector actuation developed by Evans and Stroup permit quantitative estimation of detection time lags for thermally actuated devices. These models use the Response Time Index (RTI) characterizations of heat detector reaction developed by Heskestad and Smith.[15] The DETACT-QS model[13] uses Alpert's quasi-steady correlations; it does not incorporate a transport time lag. The DETACT-T2 model[14] uses the t-squared correlations of Heskestad and Delichatsios, which incorporate the transport time lag represented by Equation 23. Analytical solutions of the detector response equations using the t-squared correlations have been developed by Beyler;[7] these also incorporate the transport lag.

Suppression Time Lags

The suppression time lag is fairly easy to assess for buildings with automatic suppression systems, but it's more difficult to consider where reliance is placed on manual suppression. For wet pipe sprinkler systems, the suppression time lag should be nil; water application begins immediately upon actuation of a sprinkler. This does not imply that the rate of water discharge will be adequate for fire control. A separate analysis is required to determine the adequacy of the water application rate; the discharge rate needed will depend on the transport and detection lag periods as well as on the rate of fire growth. The relationships between sprinkler actuation sensitivity and the required discharge density for effective fire control have been and continue to be explored in connection with the development of the Early Suppression Fast Response (ESFR) and Quick Response Sprinkler (QRS) technologies.

The suppression time lag for dry-pipe sprinkler systems can be

evaluated by actual test; it should not exceed one minute at the most remote sprinkler if the system conforms with the intent of NFPA 13,[16] although for systems with a piping capacity of less than 750 gallons, the sprinkler standard does not require this performance. In recognition of the impact of the suppression time lag on the potential for fire control, NFPA 13 requires that dry systems be designed for an area of operation 30% larger than for wet systems. Nonetheless, the better performance record of wet systems[17] is undoubtedly related to their reduced suppression lag times.

Suppression lags associated with manual suppression can be at least five minutes under good circumstances. Usually, it will be even longer before effective fire suppression activity commences. For example, under ideal conditions a capable urban fire department may be notified and respond within five minutes to a building fire. But it will take more time to evaluate the situation, make attack decisions, hook engines to hydrants, pull hoses to the fire floor, and ultimately put water effectively on the fire. Any uncertainty with respect to fire department notification and response can add significantly to this delay. In any case, typical suppression lags associated with manual fire fighting can make this protection strategy ineffective against rapidly developing fires even under optimum conditions of fire department notification and response.

Discussion

The general goal of fire mitigation strategies is to minimize the net effect of the three time lags discussed above. It is useful to consider fire growth scenarios and mitigation strategies in terms of these lag periods. This represents a convenient framework with practical physical significance; it also helps to illustrate why some fires are difficult to control, even with automatic fire suppression systems.

The transport time lag is primarily a geometric factor, although, as indicated by Equation 23, the fire growth rate has an influence on this parameter. Transport time lags are most significant in tall spaces and in spaces with thermally actuated fire detectors located at large spacings. It is not by coincidence that fires in tall spaces frequently result in high challenge fires. In such spaces, the transport time lag can be minimized through the use of line-of-sight detection devices, such as optical flame detectors, which respond to radiant energy emitted by a fire. This energy travels to the detector at the speed of light, thus eliminating the transport time lag. The detection lag for these devices is also minimal because of their sensitivity. Due to the potential for unwanted alarms with these devices, they rarely are used to actuate suppression systems automatically, so the suppression time lag still must be addressed where they are used.

The detection time lag is a function of both the fire environment and the detection device being used. For detection devices, such as sprinklers, heat detectors, and smoke detectors, that rely on the transport of buoyant gases to the ceiling for their operation, the primary environmental parameters are the heat release rate of the fire and the geometry of the space. For such devices, tall spaces have longer detection lag times than shorter spaces because of the additional entrainment of air that occurs over the additional height. According to plume theory and the available correlations, air entrainment varies as the 5/3 power of height. Coupled with the longer transport time lags for such spaces, this means the design of fire protection systems for such spaces requires special attention. In tall spaces with significant potential life safety implications, such as hotel atria, the control of combustibles to minimize the possibility of a serious fire may be the most reasonable alternative.

Examples

Two examples of t-squared fires will be considered to illustrate the potential impact of the transport, detection, and suppression time lags on the performance of fire protection systems. The first example considers "slow," "medium," "fast," and "ultrafast" t-squared fires[18] in a sprinklered space with a high ceiling, such as an atrium, an exhibition hall, or a warehouse. The second example considers the response to these same fires of a heat detection system installed in accordance with the listed spacing of the heat detectors in a large space with low ceilings, such as an open office area. The fire source is assumed to be at the floor level for both examples.

Example 1: Sprinklers in a Space with a High Ceiling

The space considered here has a ceiling height of 15.25 m (50 ft). Sprinklers with a temperature rating of 71°C and an RTI value of 150 $(ms)^{1/2}$ are spaced on a 3 m grid, representative of an ordinary hazard spacing. The maximum radial distance of a sprinkler to the plume centerline is given by:

$$r = s / \sqrt{2} = 2.1 \text{ m} \tag{35}$$

$$r/H = 2.1/15.25 = 0.14 \tag{36}$$

Assuming a fire located at floor level that develops with a theoretical heat release rate characterized as "ultrafast," this yields:

$$t_l = [0.954\,(15.25 + 2.1)] / (0.028 \times 0.188 \times 15.25)^{1/5} \text{ s} \tag{37}$$
$$= 27 \text{ s (12 s by Newman's method–Equation 25)}$$

The detection time delay, t_d, for this example is calculated to be 216 s, using the DETACT-T2 model.[14] Thus, a quasi-steady analysis would suggest sprinkler actuation at a heat release rate of 8.8 MW (αt_d^2), while a t-squared analysis yields a heat release rate at sprinkler actuation of 11.2 MW $[\alpha (t_l + t_d)^2]$, a 28% increase. The relative importance of this difference must be evaluated. For this example, the size of the fire before sprinkler actuation calculated by either analysis is perhaps of more concern than the differences between the two analyses. Nonetheless, the difference between the sensed and actual heat release rates at detection may be the difference between satisfactory and unsatisfactory sprinkler system performance and should be evaluated.

Results of similar analyses for slow, medium, and fast t-squared fires in this space are illustrated in Table 2. No suppression time lag was considered for these calculations, representative of a building with a wet pipe sprinkler system. The detection time decreases with increasing fire growth rate, but the heat release rate at detection increases with fire growth rate despite the faster detection. Similarly, the transport time lag decreases with increasing fire growth rate, but the ratio of actual to sensed heat release rates at detection increases with increasing fire growth rates.

Example 2: Heat Detectors in Large Spaces with Low Ceilings

In this example, the response of heat detectors listed for spacings of 15.25 m (50 ft) to the standardized t-squared fires is considered. Heat detectors that obtain this listed spacing commonly operate by rate-of-rise (ROR), but for the present discussion, fixed temperature detectors with ratings of 57.2°C (135°F) are assumed. This spacing and temperature rating yield an approximate RTI value[14] of 54 $(m - s)^{1/2}$. A ceiling height of 3 m is used, representative of typical office or similar commercial spaces.

The worst-case radial distance from a detector is calculated as:

$$r = s/\sqrt{2} = 10.8 \text{ m} \quad (38)$$

$$r/H = 10.8 \text{ m}/3 \text{ m} = 3.6 \quad (39)$$

Table 2. Example results for sprinklers in a 15.25 m tall space.

t^2 Growth Rate	α (W/s^2)	t_l (s)	t_d (s)	Q_s (MW)	Q_a (MW)	Q_a/Q_s
Slow	3	63	1276	4.8	5.3	1.10
Medium	12	48	670	5.4	6.2	1.15
Fast	47	36	373	6.5	7.9	1.20
Ultrafast	188	28	216	8.8	11.2	1.28

Table 3. Example results for detectors at 15.25 m spacings.

t^2 Growth Rate	α (W/s^2)	t_l (s)	t_d (s)	Q_s (MW)	Q_a (MW)	Q_a/Q_s
Slow	3	70	828	2.0	2.4	1.20
Medium	12	52	463	2.6	3.2	1.23
Fast	47	40	277	3.6	4.7	1.31
Ultrafast	188	30	172	5.6	7.7	1.38

For a fire with a theoretical heat release growth rate characterized as "fast," the transport lag is calculated as:

$$t_l = [0.954\,(3 + 10.8)] / (0.028 \times 0.047 \times 3)^{1/5}\ \text{s} \qquad (40)$$
$$= 40\ \text{s}\ (48\ \text{s by Newman's method–Equation 25})$$

For this case, a detection time of 277 seconds is calculated without the transport lag; the corresponding heat release rate is 3.6 MW. When the transport time is considered, the detection time becomes 317 seconds and the corresponding heat release rate is 4.7 MW. This represents an increase of 31 percent compared to the quasi-steady case. Results of similar calculations for the four standardized parabolic fire growth rates are tabulated in Table 3. These calculations show the same trends that are found in the first example.

These examples help to illustrate the potentially important role of the transport lag in the response of fire detection devices that rely on the transport of buoyant gases to and across the ceiling. Care must be exercised in the application of quasi-steady models of detector response, which do not consider the influence of this transport lag.

Summary

The relationship between quasi-steady and power law data correlations for fire plumes and ceiling jets has been discussed. Available correlations reduce to the same form, once a transport time lag is considered. The roles of this transport lag, a detection lag, and a suppression lag on the development and suppression of building fires have been considered. The evaluation of fire protection strategies can be considered in terms of these three time lags.

Methods to evaluate existing or proposed fire protection strategies in terms of the three lag periods have been presented for large spaces with flat, unobstructed ceilings. In many spaces, particularly tall ones and spaces with large detector spacings, traditional thermally actuated fire

detection and suppression systems may not provide an adequate level of protection. These systems may not provide fire control or suppression before an unacceptable hazard develops. In such spaces, a number of alternative fire protection strategies can be considered:

1. The use of more fire resistant materials and products to reduce the rates of fire growth and hazard development;

2. The use of fire detection devices that do not rely upon the transport and detection of thermal fire signatures;

3. The use of automatic suppression systems to minimize suppression lag times.

The expected effectiveness of these alternatives can be evaluated separately and jointly by the methods discussed here.

Nomenclature

A	$g/(c\,p_o\,T_o)$ (0.028 m^2/kg or $m^4/kW\,s^3$)
c	Specific heat of air (kJ/kg – K)
d	Distance traveled by fire gases (m)
D	Nondimensional distance parameter
dT	Temperature rise above ambient (K)
dT^*	Nondimensional temperature rise above ambient $[gH^{5/3}/(AQ)^{2/3}]\,(dT/T_o)$
g	Gravitational constant (9.8 m/s^2)
H	Height above plume source (m)
k_T	Plume/ceiling jet temperature coefficient ($K - m^{5/3}/kW^{2/3}$)
k_u	Plume/ceiling jet velocity coefficient ($m^{4/3}/s - kW^{1/3}$)
p	Fire growth exponent
p_o	Density of air (kg/m^3)
Q	Total heat release rate of fire (kW)
r	Radial distance from fire axis (m)
s	Detector or sprinkler spacing (m)
t	Time (s)
t_o	Incubation time offset (s)
t^*	Nondimensional time
T	Temperature (K)
$\overline{u}$	Average velocity of fire gases (m/s)
U	Fire gas velocity (m/s)
U^*	Nondimensional velocity $[H/(AQ)]^{1/3}\,U$
z	Coordinate above plume source
α	Power law fire growth coefficient (kW/s^p)

Subscripts

a	Actual
c	Convective
cj	Ceiling jet
crit	Critical
d	Detection lag
f	Pertaining to the heat front
l	Transport lag
o	Ambient
pl	Plume
s	Sensed, suppression lag
sup	Suppression
t	theoretical
tot	Total

References

1. Alpert, R.L., "Calculation of Response Time of Ceiling-mounted Fire Detectors," *Fire Technology*, **8**, 1972, pp. 181-195.
2. Heskestad, G. and Delichatsios, M.A., "The Initial Convective Flow in Fire," *Seventeenth Symposium (International) on Combustion*, The Combustion Institute, Pittsburgh, pp. 1113–1123.
3. Alpert, R.L. and Ward, E.J., "Evaluation of Unsprinklered Fire Hazards," *Fire Safety Journal*, **7**, 1984, pp. 127–143.
4. Beyler, C.L., "Fire Plumes and Ceiling Jets," *Fire Safety Journal*, **11**, 1986, pp. 53–75.
5. Morton, B.R., Taylor, J.S., and Turner, G.I., "Turbulent Gravitational Convection from Maintained and Instantaneous Sources," *Proceedings of the Royal Society*, Vol. A234, London, 1956, pp. 1–23.
6. Alpert, R.L., "Turbulent Ceiling Jets Induced by Large-Scale Fires," *Combustion Science and Technology*, **11**, 1975, pp. 197–213.
7. Beyler, C.L., "A Design Method for Flaming Fire Detection," *Fire Technology*, **20**, No. 4, 1984, pp. 5–16.
8. Heskestad, G. and Delichatsios, M.A., "Update: The Initial Convective Flow in Fire," to appear in *Fire Safety Journal*.
9. Tewarson, A., "Generation of Heat and Chemical Compounds in Fires," *The SFPE Handbook of Fire Protection Engineering* (P.J. DiNenno, Editor-in-Chief), National Fire Protection Association, Quincy, MA, 1988, pp. 1–179 - 1–199.
10. Johnson, J.E., "Concepts of Fire Detection," Pyrotronics, Inc., Cedar Knolls, NJ, 1970, p. 1.
11. Newman, J.S., "Principles for Fire Detection," *Fire Technology*, **24**, No. 2, 1988, pp. 116–127.
12. Newman, J.S., "Prediction of Fire Detector Response," *Fire Safety Journal*, **12**, 1987, pp. 205–211.

13. Evans, D.D., and Stroup, D.W., "Methods to Calculate the Response Time of Heat and Smoke Detectors Installed Below Large Unobstructed Ceilings," *Fire Technology*, **22**, No. 1, 1985, pp. 54–65.
14. Stroup, D.W. and Evans, D.D., "Use of Computer Fire Models for Analyzing Thermal Detector Spacing," *Fire Safety Journal*, 14, 1988, pp. 33–45.
15. Heskestad, G. and Smith, H.F., "Investigation of a New Sprinkler Sensitivity Approval Test: The Plunge Test," *Technical Report Serial No. 22485. RC 76-T-50*, Factory Mutual Research Corp., Norwood, MA, 1976.
16. Standard for the Installation of Sprinkler Systems, *NFPA 13-1987*, National Fire Protection Association, Quincy, MA, 1987.
17. "Automatic Sprinkler Performance Tables, 1970 Edition," *Fire Journal*, 64, No. 4, 1970.
18. Standard on Automatic Fire Detectors, *NFPA 72E-1987*, National Fire Protection Association, Quincy, MA, 1987.